

# Effects of Solvent Type on Low-Temperature Sintering of Silver Oxide Paste to Form Electrically Conductive Silver Film

INYOUNG KIM<sup>1</sup> and SANGKI CHUN<sup>2,3</sup>

1.—Printed Electronics Research Center, Korea Institute of Machinery and Materials, 104 Sinsongno, Yuseong-gu, Daejeon 305-343, Korea. 2.—Information Technology & Electronic Materials Institute, LG Chem Research Park, 104-1, Moonji-dong, Yuseong-gu, Daejeon 305-380, Korea. 3.—e-mail: sangki@lgchem.com

Silver oxide pastes were formulated from silver oxide powder, silver  $\alpha$ -neodecanoate, and solvents, which lowers the sintering temperature of printed silver films to 150°C. In this paper, solvent effects were investigated through the formulation of silver oxide pastes using various solvents with high boiling points such as glycol, ether, and terpineol. Solvent structures such as terminal methyl and alkoxy groups affected the solubility of silver  $\alpha$ -neodecanoate and the swelling of the polydimethylsiloxane (PDMS) blanket. Particularly, higher solubility induced uniform mixing of the silver oxide powder and silver  $\alpha$ -neodecanoate, which resulted in higher conductivity after sintering. Glycols and monoalkyl ethers reacted with the silver oxide or silver salt, which deteriorated the pot life of the paste. Among the various candidates,  $\alpha$ -terpineol satisfied all the requirements such as printability and stability, exhibiting a solubility of 47.8 g in 100 g of solvent, PDMS swelling of 4.6%, and conductivity of  $1.8 \times 10^5$  S/cm after sintering at 150°C for 30 min.

**Key words:** Ink formulation, low-temperature sintering, roll-to-roll printing, silver  $\alpha$ -neodecanoate, silver oxide pastes

## INTRODUCTION

Printing technology for the fabrication of functional electronic devices, so-called printed electronics, is in the spotlight as a newly emerging technology because of its ecofriendly and cost-effective benefits. In recent years, traditional printing methods, mainly inkjet and screen printing as well as gravure, offset, and flexographic printing, have been applied to the development of touch panels, solar cells,<sup>1–3</sup> flexible displays,<sup>4,5</sup> thin-film transistors,<sup>6–11</sup> and smart labels.<sup>12</sup> Among these printing methods, gravure, offset, and flexographic printing are commonly employed as roll-to-roll methods and thus have the advantage of mass production. In particular, high aspect ratios and high resolution are increasingly important issues in

printing techniques, enabling manufacturers to replace indium tin oxide (ITO) films in touch panels with low-priced metal electrodes and to improve the power conversion efficiency of solar cells.<sup>13–15</sup>

The paste material is obviously one of the most important factors influencing the electrical conductivity and printing quality. Recently, for flexible devices, organic films such as polyethylene terephthalate (PET), polyethylene naphthalate (PEN), and polyimide (PI) films have been used as substrates for printed devices.<sup>4–12</sup> Therefore, there has been strong demand for paste with a sintering temperature below the glass-transition temperatures of such organic substrates.<sup>16,17</sup> For this low-temperature sintering, the use of nanoparticles has been the focus of paste study, owing to their advantages of large surface area ( $A$ ) and surface energy ( $\gamma$ ).<sup>18–20</sup> Generally, the driving force for sintering is the reduction of the total interfacial energy:  $\Delta(\gamma A) = \Delta\gamma A + \gamma\Delta A$ .<sup>20</sup> Therefore, reduction

(Received October 9, 2010; accepted June 7, 2011; published online July 6, 2011)

of particle size can increase the driving force for sintering, which effectively functions to lower the sintering temperature.<sup>21</sup> Silver nanoinks for inkjet printing have been reported to have a resistivity of  $\sim 3 \mu\Omega \text{ cm}$  after sintering at  $250^\circ\text{C}$ ,<sup>16,17</sup> and Buffat reported that the size of gold particles also affected the melting point.<sup>21</sup> However, this low-temperature sintering makes it more problematic to achieve other material performance and reliability requirements for device applications.<sup>16,17,20</sup> To transcend this limitation, ink formulation becomes as important as the synthesis of nanoparticles. In particular, the solvent used in the paste has decisive effects on the sintering temperature, the stability of the paste, as well as its printability. However, very few approaches such as ink formulation or investigation of solvent effects for low-temperature sintering have been presented.<sup>22,23</sup>

Honda et al.<sup>22,23</sup> demonstrated a novel idea for low-temperature sintering of silver oxide pastes using nanosized silver oxide powder and silver metallorganic compounds. The mixture of silver oxide powder and silver metallorganic compounds has shown excellent processability as well as high conductivity after thermal treatment. Chun et al.<sup>24</sup> suggested the use of silver oxide pastes with silver alkanoate for roll-to-roll printing, and their films printed on a PET substrate could be sintered at  $150^\circ\text{C}$ . The conductivity of the silver oxide pastes was found to depend upon the linear chain length  $n$  of the silver salt,  $\text{AgOCO-C}(\text{CH}_3)_2\text{-(CH}_2)_n\text{-CH}_3$ . However, it is still necessary to explore how the silver salt works with other components in the paste during sintering, and how the silver oxide pastes are transformed into silver films. Especially, the solvent in the paste has decisive effects on the stability of the paste, its printability, and its sintering temperature. Moreover, in a mixture of silver oxide powder and silver metallorganic compounds, the solubility of the silver metallorganics can also influence the dispersion. The solvent should not degrade the roll-blanket materials or paste stability in the short term, i.e., the solvent should not interact with other components or materials in the paste before sintering. As an ongoing part of silver oxide paste research, in this study, the effects of solvent variation on paste properties were evaluated and the optimum solvent for silver oxide paste is suggested. To perform a thorough and systematic investigation, our focus of experimentation was on the following: (1) the solubility of silver neodecanoate, (2) the swelling of the roll blanket made of polydimethylsiloxane (PDMS), (3) the interaction with silver oxide, (4) conductivity, (5) microstructure, and (6) the fluidity of the paste.

## EXPERIMENTAL PROCEDURES

As solvents for silver oxide paste, dipropylene glycol (DPG), triethylene glycol (TEG), tetraethylene glycol (TTEG), diethylene glycol monobutyl

ether (DEGBE), dipropylene glycol monomethyl ether (DPGME), dipropylene glycol monobutyl ether (DPGBE), tripropylene glycol monomethyl ether (TPGME), tripropylene glycol monopropyl ether (TPGPE), tripropylene glycol monobutyl ether (TPGBE), diethylene glycol dibutyl ether (DEGDDE), dipropylene glycol dimethyl ether (DPGDME), triethylene glycol dimethyl ether (TEGDME), tetraethylene glycol dimethyl ether (TTEGDME), and  $\alpha$ -terpineol were purchased from Aldrich and used as received. Granular silver oxide powder was purchased from Kojundo, Japan. Sylgard 184 silicone, a two-part PDMS elastomer, was purchased from Dow Corning. For solid PDMS, a 10:1 mixture of base and curing agent was mixed and degassed under vacuum and cured at room temperature for 24 h.

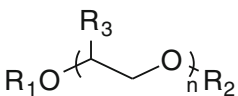
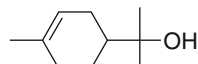
The silver salt was synthesized following modified procedures, as described by Vest<sup>25</sup> and Smith.<sup>26</sup> Aqueous sodium hydroxide solution was slowly added to an equimolar amount of neodecanoic acid in methanol and stirred for 1 h. If needed for neutralization, diluted nitric acid was added to adjust the pH to 7. Then, an equimolar amount of aqueous silver nitrate was added and stirred for 1 h to produce a white precipitate of silver neodecanoate. The precipitate was collected by filtration and washed with distilled water and methanol. Then, it was dried in a vacuum oven overnight.

The silver oxide pastes used in this study were prepared by mixing silver oxide powder (Kojundo, Japan) and  $\alpha$ -silver neodecanoate in solvent. All materials were mixed for 2 min and degassed for 1 min using a planetary mixer (AR-250; Thinky, Japan). Subsequently, uniform pastes were prepared using a triple-roller grinder (Exakt 50, Germany), which breaks agglomerates of silver(I) oxide particles. Their mixing mass ratio was 4:4:2 silver oxide powder,  $\alpha$ -silver neodecanoate, and solvent, as based on our previous results.<sup>24</sup> Each solvent listed in Table I was used for the silver oxide paste, and their viscosity was measured using a conventional rheometer (Brookfield DV-III Ultra, Germany).

The silver oxide paste was coated onto a PET film with a thickness of  $30 \mu\text{m}$  using a wire-wound rod coater<sup>27</sup> and cured at  $150^\circ\text{C}$  for 30 min. The four-point probe method<sup>28</sup> (ASP probe, MCP-TP03P and Mitsubishi Chemical, MCP-T600, Japan) was used to measure the sheet resistance of the silver film,  $R_s$ . The thickness,  $t$ , of the silver films was measured using a Teclock thickness gauge following JIS K6783. The electrical resistivity,  $\rho$ , of the Ag films was calculated as  $\rho = R_s \times t$ . Three samples were tested and averaged for each paste composition. The microscopic morphologies of the silver films were observed under a field-emission scanning electron microscope (s-4800; Hitachi, Japan).

Typically, an excess amount of silver neodecanoate was dissolved in the solvent to obtain a saturated solution, which was then filtered through a

**Table I. Solvent structure, boiling point, solubility of silver  $\alpha$ -neodecanoate, swelling ratio of PDMS, and exhibition of the silver mirror reaction**

No.	Solvent	Structure			Boiling Point (°C)	Solubility (g/100 g)	Swelling (%)	Occurrence of Silver Mirror Reaction	
		<i>n</i>	R1	R2					R3
									
1	Dipropylene glycol	2	H	H	CH <sub>3</sub>	275	0.06	0.9	Yes
2	Triethylene glycol	3	H	H	H	285	0.64	0.7	Yes
3	Tetraethylene glycol	4	H	H	H	327	0.71	0.5	Yes
4	Diethylene glycol monobutyl ether	2	C <sub>4</sub> H <sub>9</sub>	H	H	231	26.5	1.6	Yes
5	Tripropylene glycol monopropyl ether	3	C <sub>3</sub> H <sub>7</sub>	H	CH <sub>3</sub>	261	27.5	4.1	Yes
6	Tripropylene glycol monomethyl ether	3	CH <sub>3</sub>	H	CH <sub>3</sub>	243	30.7	4.1	Yes
7	Tripropylene glycol monobutyl ether	3	C <sub>4</sub> H <sub>9</sub>	H	CH <sub>3</sub>	276	33.9	4.0	Yes
8	Dipropylene glycol monomethyl ether	2	CH <sub>3</sub>	H	CH <sub>3</sub>	188	37.2	6.2	Yes
9	Dipropylene glycol monobutyl ether	2	C <sub>4</sub> H <sub>9</sub>	H	CH <sub>3</sub>	227	39.9	2.3	Yes
10	Triethylene glycol dimethyl ether	3	CH <sub>3</sub>	CH <sub>3</sub>	H	216	29.8	2.7	No
11	Tetraethylene glycol dimethyl ether	4	CH <sub>3</sub>	CH <sub>3</sub>	H	275	38.5	1.4	No
12	Diethylene glycol dibutyl ether	2	C <sub>4</sub> H <sub>9</sub>	C <sub>4</sub> H <sub>9</sub>	H	256	43.5	17.1	No
13	Dipropylene glycol dimethyl ether	2	CH <sub>3</sub>	CH <sub>3</sub>	CH <sub>3</sub>	175	47.9	21.9	Yes
14	$\alpha$ -Terpineol					220	47.8	4.6	No
									

Solubility is the maximum equilibrium amount of solute that can dissolve per 100 g solvent. Swelling is the percentage of expanded PDMS mesh patterns by solvent.<sup>27</sup>

0.45- $\mu$ m membrane filter. The ultraviolet absorbance of the filtered solution was measured from 210 nm to 220 nm. This was performed after forming a 100-fold dilution by mixing a 100- $\mu$ L aliquot of the filtered solution with 10 mL of solvent. Absorbance data were referenced to that obtained with a solution of 50 mg silver neodecanoate in 10 mL of solvent.

Swelling of PDMS was defined as

$$\text{Swelling (\%)} = (L - L_0)/L_0 \times 100,$$

where  $L_0$  and  $L$  are the original length and the expanded length of PDMS mesh patterns after swelling, respectively. Therefore, swelling was measured by comparing the pitch width of PDMS mesh patterns before and after immersion in the solvent.<sup>29</sup> The patterned PDMS sheet was made by molding and curing.<sup>29</sup> The dimensions of the mesh were 300  $\mu$ m pitch and 1 mm thick. The PDMS pieces were punched in the shape of a circle and immersed in each solvent for 24 h at 25°C. The pitch width of the PDMS mesh pattern was measured using a Keyence VF-7510 profile micrometer. Two samples for each solvent were tested and averaged. For each sample, two different positions were selected and measured.

## RESULTS AND DISCUSSION

The silver oxide pastes were formulated from silver oxide powder, silver  $\alpha$ -neodecanoate, and solvent. To examine the effect of solvent structure on the paste's properties, various candidate solvents for the silver oxide pastes with high boiling points were investigated and are listed in Table I. Solvents with high boiling points were selected because a low boiling point is not conducive to maintaining uniform quality of the paste during printing due to the easy evaporation of the solvent. No additional binders or additives were added to the silver oxide paste. The basic solvent structures listed in Table I are  $R_1-(CHR_3-CH_2-O)_n-R_2$ , where  $R_1$  and  $R_2$  are the functional groups at the terminal points and  $-(CHR_3-CH_2-O)_n-$  is the repeating chain unit with a chain length of  $n$  in the solvent structure. The solvents can be classified into small groups of alcohol, glycol, and ether based on  $R_1$  and  $R_2$ .

The solubility of silver  $\alpha$ -neodecanoate in solvent was investigated as shown in Table I, because the solubility of silver  $\alpha$ -neodecanoate can affect the uniform mixing of the paste, which is closely related to the uniform dispersion of silver oxide powder in the paste and the thixotropy of the silver oxide paste. In this study, solubility was defined as the

maximum equilibrium amount of a solute that could dissolve per 100 g of solvent. The solvent groups in Table I follow a certain trend in solubility. Glycols **1–3** with hydroxyl groups -OH at both terminals  $R_1$  and  $R_2$  showed low solubility, below 0.71, regardless of the chain length  $n$ . However, ether groups **4–13** with one or two alkoxy groups at  $R_1$  and  $R_2$  showed conspicuously high solubility of 26 to 47. The more alkoxy groups at the terminals, the higher the solubility. Moreover,  $\alpha$ -terpineol **14**, with three methyl terminal groups, revealed the highest solubility of 47.8. Solubility is determined by the balance of intermolecular forces between the solvent and the solute.<sup>30–32</sup> In particular, the polarity of functional groups can be understood intuitively from the difference in the electronegativity between atoms. -OH is a representative example of a polar bond, giving polarity to methanol or water.<sup>33</sup> On the other hand, -CH<sub>3</sub> can be understood as a nonpolar bond.<sup>33</sup> The solute in this study, silver  $\alpha$ -neodecanoate, AgOCO-C(CH<sub>3</sub>)<sub>2</sub>-(CH<sub>2</sub>)<sub>5</sub>-CH<sub>3</sub>, has several methyl groups and hydrocarbon chains with silver functional groups. AgOCO- may show some degree of polarity, but the main body of the methyl groups and hydrocarbon chains can show nonpolarity.<sup>34</sup> Therefore, to dissolve the silver  $\alpha$ -neodecanoate, the solvent should be nonpolar and the methyl groups of solvents can be very helpful to increase solubility. From this point of view, the glycols **1–3** in Table I with hydroxyl bonds -OH at both terminal points are not good for dissolving silver  $\alpha$ -neodecanoate because they have high polarity, as does ethanol.<sup>34</sup> In the case of ethers **4–13** in Table I, instead of the hydroxyl functional groups, the solvents have alkoxy groups at the terminal points of the solvent, which are favorably towards the solubility of the solvent.  $\alpha$ -Terpineol **14** in Table I shows the highest solubility, with three methyl functional groups. The two carbon bridges between the ether oxygens, the main structure of the solvents in Table I, is a typical chain structure of crown ether, which has regularly shown complexation with alkali and alkaline earth metal salts.<sup>35–40</sup> In the study of open chain analogs of crown ether podands, adequate lipophilicity was required for useful application of liquid membranes or organic solvents as phase-transfer agents,<sup>41,42</sup> and the lipophilicity can be regulated by attaching either aromatic residues or methyl pendants to the podand.<sup>43</sup> This also explains that the solubility trends in Table I could originate from the change in lipophilicity. In the case of the bridge effect in podands, the formation of metal complexes was affected by the type of bridge such as (CH<sub>2</sub>CH<sub>2</sub>)<sub>2</sub>O, (CH<sub>2</sub>)<sub>3</sub>, and (CH<sub>2</sub>)<sub>2</sub>, which was explained with a three-dimensional, "wrap-around" coordination of the metal cation.<sup>44</sup> In Table I, monoalkyl ether groups **4–9** and dialkyl ether groups **10–13** show different trends of solubility of silver  $\alpha$ -neodecanoate. In the monoalkyl ether groups **4–9**, where only  $R_1$  is replaced by an alkoxy group, the effect of the length  $n$  of the -(CH<sub>3</sub>)CHCH<sub>2</sub>O- chain can be recognized by

comparing **6** (solubility 30.7) with **8** (solubility 37.2), and **7** (solubility 33.9) with **9** (solubility 39.9), respectively. This means that, the shorter the chain length, the higher the solubility of the organic silver salt. On the other hand, in the dialkyl ether groups **10–13**, another trend is observed for the -(CH<sub>2</sub>)<sub>2</sub>O-chain. Comparing **10** (solubility 29.8) with **11** (solubility 38.5), the higher solubility is a result of the longer chain length. Initially, the hydrocarbon chain of -CH<sub>2</sub>- shows nonpolar nature; therefore, it plays a role of reducing the polar effect of the terminal group, similar to the way in which the polarity of alcohols decreases with the carbon chain length.<sup>34</sup> Similarly, the effect of the -(CH<sub>2</sub>)<sub>2</sub>O- chain can be observed in ethylene glycol. With an increase of the -(CH<sub>2</sub>)<sub>2</sub>O- chain, the polarity of the ethylene glycol decreases slightly.<sup>34</sup> Therefore, a longer -(CH<sub>2</sub>)<sub>2</sub>O- chain can reduce the polarity of dialkyl ether and facilitate complex formation with silver, which results in higher solubility of silver  $\alpha$ -neodecanoate. On the other hand, the -CH(CH<sub>3</sub>)CH<sub>2</sub>O- chain can have higher polarity than -(CH<sub>2</sub>)<sub>2</sub>O- because of the structural asymmetry. Moreover, in the case of monoalkyl ether, one of the terminal groups has a -OH group, so the asymmetric structure of ether can induce a higher polarity than for dialkyl ether. The shorter chain length of -CH(CH<sub>3</sub>)CH<sub>2</sub>O- is rather helpful in reducing the polarity of the solvent and increasing the solubility.

In gravure-offset printing, PDMS is usually used for the roll-blanket material, so that the solvent must not have a rapid chemical or physical interaction with PDMS. Specifically, swelling of PDMS by the solvent can cause serious damage to the printing quality and the lifetime of the PDMS roll. Table I also presents the swelling of PDMS for each solvent, defined as the percentage expanded length of PDMS mesh patterns.<sup>29</sup> Glycols **1–3**, with very low solubility, have low swelling rates of 0.5% to 0.9%. However, ethers **4–13**, having higher solubility than glycols, exhibit a wide range of swelling from 1.6% to 21.9%. In particular, diethylene glycol dibutyl ether **12** and dipropylene glycol dimethyl ether **13**, which rank the highest in solubility at 43.5 and 47.9, also show the highest swelling at 17.1% and 21.9%, respectively. The rest show lower swelling, below 6.2%. This result reveals that the swelling of PDMS exhibits a similar tendency to the solubility in the solvent. Although the relationship between  $\delta$  and swelling is not linear and differs for each solvent system, it is expected that a solvent with  $\delta$  similar to that of PDMS will swell PDMS.<sup>45–48</sup> This is not surprising considering that solubility is measured by the degree of swelling of materials such as cross-linked polymers that do not dissolve.<sup>43–46</sup> It was also found that a solvent with high swelling of PDMS showed high solubility.<sup>29</sup> PDMS has a low dipole moment, i.e., low polar properties,<sup>45</sup> so nonpolar solvents such as benzene, pentane, cyclic hydrocarbons, aromatic hydrocarbons, halogenated compounds, and ethers (diethyl

ether, dimethoxyethane, tetrahydrofuran) revealed high solubility and high swelling.<sup>29</sup> In Table I, the low swelling of the glycols 1–3 may be due to their high polarity. Most alcohols such as 1-propanol, ethanol, methanol, phenol, ethylene glycol, and glycerol were reported to have low solubility and therefore did not cause the PDMS to swell.<sup>49,50</sup>

Some solvents showed reduction of silver salt into silver to form a silver mirror on the clean glass vessel. The solvent, including ketone or aldehyde, can reduce the silver salt or silver oxide powder in the paste to silver. While maintaining the high solubility of silver  $\alpha$ -neodecanoate and low swelling of PDMS, the solvent should also not reduce the silver salt or silver oxide to silver according to this so-called silver mirror reaction. Fourteen kinds of candidate solvent were examined for the silver mirror reaction, and glycols 1–3 and monoalkyl ethers 4–9 were positive for the silver mirror reaction, as summarized in Table I. The hydroxyl radical in the primary alcohols can be transformed to ketone or aldehyde forms, so reduction reactions of silver  $\alpha$ -neodecanoate with glycol and monoalkyl ethers may occur. However, in the case of  $\alpha$ -terpineol 14, the hydroxyl functional group -OH cannot be transformed into other forms. Thus, it is stable enough to prevent the silver mirror reaction with silver  $\alpha$ -neodecanoate. Only four solvents among the candidates in Table I do not exhibit the silver mirror reaction.

Among the solvents free from the silver mirror reaction, only three had solubility higher than 30. Using these three solvents ( $\alpha$ -terpineol 14, tetraethylene glycol dimethyl ether 11, and diethylene glycol dibutyl ether 12), silver oxide pastes were formulated. Each silver oxide paste was sintered at 150°C for 10 min to 30 min. Figure 1 shows the conductivity of the printed silver oxide pastes using the three different solvents with their sintering times.  $\alpha$ -Terpineol 14 revealed a saturated conductivity ( $1.76 \times 10^5$  S/cm) after 20 min, but tetraethylene glycol dimethyl ether 11 does so after 25 min. In the case of diethylene glycol dibutyl ether 12, it continues to increase after 30 min. The change in conductivity reveals a direct dependence on the solubility of the silver  $\alpha$ -neodecanoate. Higher solubility induced uniform mixing of the silver oxide powder and silver  $\alpha$ -neodecanoate, which resulted in higher conductivity after sintering. Similar results for the solubility, depending on the  $-\text{CH}_2-$  chain length in the silver salt,  $\text{AgOCO-C}(\text{CH}_3)_2-(\text{CH}_2)_n-\text{CH}_3$ , were found in previous work.<sup>24</sup> The paste made with  $\alpha$ -terpineol, which has the highest solubility of 47.9, showed the best conductivity of  $1.8 \times 10^5$  S/cm after 30 min of sintering, being comparable to that of silver nanoink sintered at 170°C to 200°C.<sup>16–19</sup> The silver nanoink showed a conductivity of  $6.7 \times 10^4$  S/cm after sintering at 150°C for 30 min, being several times lower than that of silver oxide paste.<sup>17</sup>

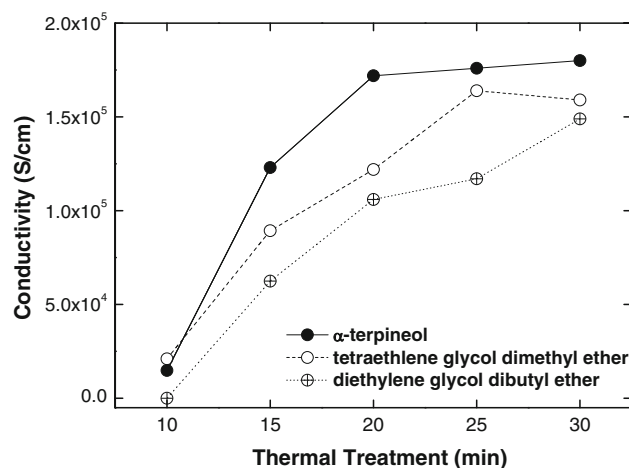


Fig. 1. Conductivity changes of silver oxide pastes with sintering time. Silver oxide pastes were formulated using three different solvents:  $\alpha$ -terpineol, tetraethylene glycol dimethyl ether, and diethylene glycol dibutyl ether. The mixing ratio of silver oxide, silver  $\alpha$ -neodecanoate, and solvent was 4:4:2 by weight, and the sintering temperature was 150°C.

This conductivity change was also closely related to the microstructural development, as shown in Fig. 2. Figure 2a shows as-dried silver oxide paste consisting of granular silver oxide powder with a diameter of  $\sim 1.5 \mu\text{m}$  and rod-shaped silver  $\alpha$ -neodecanoate with a length of  $\sim 3.2 \mu\text{m}$ . The silver oxide paste was dried at 50°C for 5 h in a convection oven. Figure 2b shows that silver oxide powder and silver  $\alpha$ -neodecanoate are reduced to silver after sintering at 150°C for 10 min. The reduction of silver oxide powder to silver was also analyzed using x-ray diffractometry (XRD).<sup>24</sup> The reduced silver particles are shown in Fig. 2b, which grow up to  $\sim 50$  nm, although necking of silver particles is not yet observed. Therefore, the conductivity still shows a low value of  $1.48 \times 10^4$  S/cm. It should be noted that the scale bar in Fig. 2a is 20 times longer than those in Fig. 2b–f. After 15 min (Fig. 2c), neck formation of silver particles was observed and open pores were generated. This necking can induce noticeable improvement of conductivity, as shown in Fig. 1. The amount of open pores, which were usually observed in the intermediate stage of sintering,<sup>20</sup> slightly increases without grain growth in Fig. 2d, e, which is reflected in a small improvement in conductivity. After 30 min, silver grains grow to a diameter of  $\sim 100$  nm and the open pores develop into closed pores, indicating that densification of the silver film has progressed.<sup>20</sup> The relationship between conductivity and microstructure in Figs. 1 and 2 illustrates that necking plays a critical role in the improvement of conductivity, rather than grain growth and densification processes, which agrees well with other reports regarding sintering of silver nanoparticles.<sup>16,17</sup>

Generally, viscosity is considered one of the main factors classifying paste applications. The pastes

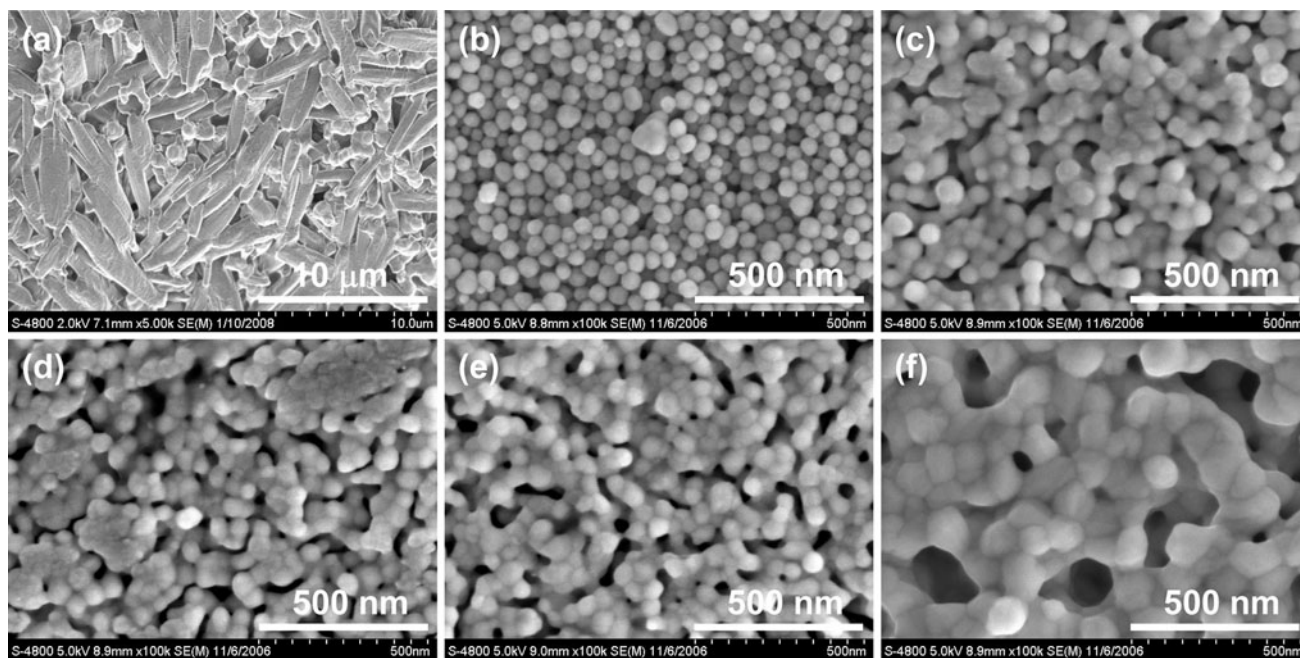


Fig. 2. SEM micrographs of silver oxide paste: (a) as-dried, and sintered at 150°C for (b) 10 min, (c) 15 min, (d) 20 min, (e) 25 min, and (f) 30 min.  $\alpha$ -Terpineol was used as the solvent, and the mixing ratio of silver oxide, silver  $\alpha$ -neodecanoate, and  $\alpha$ -terpineol was 4:4:2 by weight.

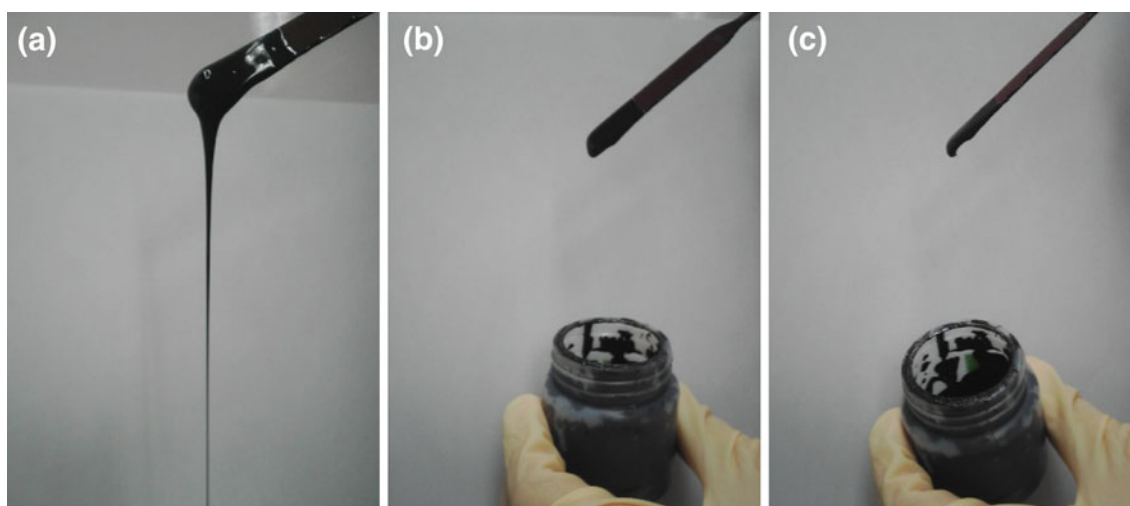


Fig. 3. Fluidity tests for silver oxide pastes formulated with (a)  $\alpha$ -terpineol, (b) tetraethylene glycol dimethyl ether, and (c) diethylene glycol dibutyl ether. The snapshot was taken at 1/60 s using a typical digital camera.

formulated using solvents **14**, **11**, and **12** in Table I revealed a viscosity of 52 Pa s, 36 Pa s, and 10 Pa s, respectively, which are suitable values for soft gravure or gravure-offset printing. Besides viscosity, the thixotropy of the paste, which indicates the fluidity of the paste during printing, is more critical for practical use of formulated pastes. To test the fluidity of the silver oxide pastes, the simple and useful method shown in Fig. 3 was used in this study. In contrast to the viscosity results, only  $\alpha$ -terpineol, which has a higher viscosity of 52 Pa s, exhibited good paste fluidity, as shown in Fig. 3a. However, no fluidity at all can be observed for the

silver oxide pastes formulated with solvents **11** and **12**, which means that these two pastes cannot be applied in the soft gravure printing process.

## CONCLUSIONS

Examinations performed on solvents were as follows: (1) solubility of silver  $\alpha$ -neodecanoate, (2) swelling of PDMS, (3) silver mirror effect, (4) conductivity, (5) microstructure, and (6) fluidity of the paste. Regarding solubility of  $\alpha$ -neodecanoate, several glycol dialkyl ethers and  $\alpha$ -terpineol showed high solubility of above 40 g in 100 g of solvent.

Methyl and alkoxy groups at the terminals of the solvent helped improve solubility. Among the solvents with high solubility, diethylene glycol dibutyl ether and dipropylene glycol dimethyl ether, each ranking highest in terms of solubility, showed the highest swelling of PDMS, 17.1% and 21.9%, respectively. In the interaction with silver  $\alpha$ -neodecanoate or silver oxide powder, all glycol and glycol monoalkyl ethers exhibited silver mirror reactions. Finally, the three candidates  $\alpha$ -terpineol, tetraethylene glycol dimethyl ether, and diethylene glycol dibutyl ether were examined for their printability using the viscosity and simple fluidity test, and only  $\alpha$ -terpineol fulfilled all the required conditions. Silver oxide paste formulated with  $\alpha$ -terpineol showed a conductivity of  $1.8 \times 10^5$  S/cm after sintering at 150°C for 30 min.

### ACKNOWLEDGEMENT

We are grateful to Jungwon Park for his assistance in recording the SEM images.

### REFERENCES

1. F.C. Krebs, *Sol. Energy Mater. Sol. Cells* 93, 1636 (2009).
2. F.C. Krebs, *Sol. Energy Mater. Sol. Cells* 93, 465 (2009).
3. M. Niggemann, B.I. Zimmermann, J.M. Haschke, M. Glatthaar, and A. Gombert, *Thin Solid Films* 516, 7181 (2008).
4. R. Gaudiana and C. Brabec, *Nature Photonics* 2, 287 (2008).
5. J. Weber, K. Potze-Kamloss, F. Hasse, P. Detemple, F. Voeklein, and T. Doll, *Sens. Actuators A* 132, 325 (2006).
6. A.E. Kats and J. Huang, *Annu. Rev. Mater. Res.* 39, 71 (2009).
7. M.A.M. Leenen, V. Arning, H. Thiem, J. Steiger, and R. Anselmann, *Phys. Status Solidi A* 206, 588 (2009).
8. Y. Li, Y. Wu, and B.S. Ong, *J. Am. Chem. Soc.* 127, 3266 (2005).
9. Y. Li, Y. Wu, and B.S. Ong, *J. Am. Chem. Soc.* 129, 1862 (2007).
10. J. Perelaer, C.E. Hendriks, A.W.M. de Laat, and U.S. Schubert, *Nanotechnology* 20, 165303 (2009).
11. T. Sekitani, Y. Noguchi, U. Zschieschang, H. Klauk, and T. Someya, *Proc. Natl. Acad. Sci. USA* 105, 4976 (2008).
12. T. Sangoi, C.G. Smith, M.D. Seymour, J.N. Venkataraman, D.M. Clark, M.L. Kleper, and B.E.J. Kahn, *Dispers. Sci. Technol.* 25, 513 (2004).
13. H. Philipp, U.S. patent 0123670 A1 (2010).
14. S.S. Georgiev, *Solid-State Electron.* 51, 376 (2007).
15. M. Deguchi, T. Itagaki, and M. Usui, U.S. patent 5151373 (1992).
16. I. Kim, Y.A. Song, H.C. Jung, J.W. Joung, S.-S. Ryu, and J. Kim, *J. Electron. Mater.* 37, 1863 (2008).
17. J.-K. Jung, S.H. Choi, I. Kim, H.C. Jung, J. Joung, and Y.-C. Joo, *Phil. Mag.* 88, 339 (2008).
18. K.J. Lee, B.H. Jun, T.H. Kim, and J. Joung, *Nanotechnology* 17, 2424 (2006).
19. Y.I. Lee, I.K. Shim, K.J. Lee, and J. Joung, *Solid State Phenom.* 124–126, 1193 (2006).
20. S.-J. Kang, *Sintering*, Chap. 1 (Oxford, Burlington: Elsevier Butterworth-Heinemann, 2005).
21. P. Buffat and J.-P. Borel, *Phys. Rev.* 13, 2287 (1976).
22. T. Honda, K. Okamoto, M. Ito, and M. Endo, K. Takahashi, U.S. Patent 6942825 (2005).
23. C.-A. Lu, P. Lin, H. lin, and S.-F. Wang, *Jpn. J. Appl. Phys.* 46, 4179 (2007).
24. S. Chun, D. Grudin, S. Kim, D. Lee, S.-H. Kim, G.-R. Yi, and I. Hwang, *Chem. Mater.* 21, 343 (2009).
25. K.F. Teng and R.W. Vest, *IEEE Trans. Compon. Hybrid. Manuf. Technol.* 11, 3 (1988).
26. A.L. Dearden, P.J. Smith, D.-Y. Shin, N. Reis, B. Derby, and P. O'Brien, *Macromol. Rapid Commun.* 26, 315 (2005).
27. D.M. MacLeod, *Coatings Technology: Fundamentals, Testing, and Processing Techniques*, ed. A. Arthur, Chap. 19 (Tracton: CRC Press, 2007).
28. D.K. Schroder, *Semiconductor Material and Device Characterization*, 2nd ed., Chap. 1 (New York: John Wiley & Sons, 1998).
29. J.N. Lee, C. Park, and G.M. Whitesides, *Anal. Chem.* 75, 6544 (2003).
30. J.H. Hildebrand and R.L. Scott, *Solubility of Nonelectrolytes*, 3rd ed., Chap. 1 (New York, NY: Reinhold Publishing Company, 1949).
31. C. Hansen and A. Beerbower, *Kirk Othmer Encyclopedia of Chemical Technology*, 2nd ed. (New York, NY: Wiley-Interscience, 1971), p. 899.
32. D.L. Hertz, *Elastomerics* 118, 18 (1986).
33. J. McMurry, *Organic Chemistry*, 7th ed. (Australia: Cengage Learning, 2008).
34. C. Reichardt, *Chem. Rev.* 94, 2319 (1994).
35. C.J.J. Pedersen, *Am. Chem. Soc.* 87, 2495 (1967).
36. C.J.J. Pedersen, *Am. Chem. Soc.* 87, 7017 (1967).
37. C.J.J. Pedersen, *Am. Chem. Soc.* 92, 386 (1970).
38. C.J.J. Pedersen, *Am. Chem. Soc.* 92, 391 (1970).
39. C.J.J. Pedersen, *Am. Chem. Soc.* 36, 254 (1971).
40. C.J.J. Pedersen, *Am. Chem. Soc.* 36, 1960 (1971).
41. J. Strzelbick and R.A. Bartsch, *Anal. Chem.* 53, 1894 (1981).
42. J. Strzelbick and R.A. Bartsch, *Anal. Chem.* 53, 2251 (1981).
43. S.I. Kang, A. Czech, B.P. Czech, L.E. Stewart, and R.A. Bartsch, *Anal. Chem.* 57, 1713 (1985).
44. W. Walkowiak, S.-I. Kang, L.E. Stewart, G. Ndip, and R.A. Bartsch, *Anal. Chem.* 62, 2022 (1990).
45. N.A. Diachun, A.H. Marcus, D.M. Hussey, and M.D.J. Fayer, *Am. Chem. Soc.* S116, 1027 (1994).
46. R. Chitra and P.E.J. Smith, *Chem. Phys.* 115, 5521 (2001).
47. G.S. Simonyan, N.M. Beileryan, E.G. Pirumyan, J.-P. Roque, and B. Boyer, *Kinet. Catal.* 42, 474 (2001).
48. M. Graffeuil, J.F. Labarre, C. Leibovici, and T.J. Theophanides, *Chim. Phys. Physicochim. Biol.* 70, 1295 (1973).
49. Y. Du, Y. Xue, and H.L. Frisch, *Physical Properties of Polymers Handbook* (Woodbury, NY: AIP Press, 1996).
50. J.-L.M. Abboud and R. Notario, *Pure Appl. Chem.* 71, 645 (1999).